Myopia Control Dose Delivered to Treated Eyes by a Dual-focus Myopia-control Contact Lens

Viswanathan Ramasubramanian, BSOptom, PhD, FAAO[1]* Nicola S. Logan, PhD,[2] Susie Jones, PhD,[2] Dawn Meyer, OD,[1] Matt Jaskulski, PhD,[1] Martin Rickert, PhD,[1] Paul Chamberlain, BSc,[3] Baskar Arumugam, PhD,[3] Arthur Bradley, PhD,[3] and Pete S. Kollbaum, OD, PhD, FAAO[1]

Downloaded from http://journals.lww.com/optvissci by BhDMf5ePHKav1zEoum1tQfN4a+kJLhEZgbsIHo4XMi0hCywCX1AWnYQp/IlQrHD3i3D0OdRyi7TvSFl4Cf3VC4/OAVpDDa8KKGKV0Ymy+78= on 07/25/2023

SIGNIFICANCE: Consistent with closed-loop models of regulated eye growth, a successful dual-focus (DF) myopia-control contact lens focused a significant proportion of light anterior to the central retina in eyes of treated children viewing near and distant targets.

PURPOSE: This study examined the optical impact of a DF contact lens during near viewing in a sample of habitual DF lens wearing children.

METHODS: Seventeen myopic children aged 14 to 18 years who had completed 3 or 6 years of treatment with a DF contact lens (MiSight 1 Day; CooperVision, Inc., San Ramon, CA) were recruited and fit bilaterally with the DF and a single-vision (Proclear 1 Day; CooperVision, Inc.) contact lens. Right eye wavefronts were measured using a pyramidal aberrometer (Osiris; CSO, Florence, Italy) while children accommodated binocularly to high-contrast letter stimuli at five target vergences. Wavefront error data were used to compute pupil maps of refractive state.

RESULTS: During near viewing, children wearing single-vision lenses accommodated on average to achieve approximate focus in the pupil center but, because of combined accommodative lag and negative spherical aberration, experienced up to 2.00 D of hyperopic defocus in the pupil margins. With DF lenses, children accommodated similarly achieving approximate focus in the pupil center. When viewing three near distances (0.48, 0.31, and 0.23 m), the added +2.00 D within the DF lens treatment optics shifted the mean defocus from +0.75 to −1.00 D. The DF lens reduced the percentage of hyperopic defocus (≥+0.75 D) in the retinal image from 52 to 25% over these target distances, leading to an increase in myopic defocus (≤−0.50 D) from 17 to 42%.

CONCLUSIONS: The DF contact lens did not alter the accommodative behavior of children. The treatment optics introduced myopic defocus and decreased the amount of hyperopically defocused light in the retinal image.

Optom Vis Sci 2023;100:376–387. doi:10.1097/OPX.0000000000002021
Copyright © 2023 The Author(s). Published by Wolters Kluwer Health, Inc. on behalf of the American Academy of Optometry. This is an open-access article distributed under the terms of the Creative Commons Attribution-Non Commercial-No Derivatives License 4.0 (CCBY-NC-ND), where it is permissible to download and share the work provided it is properly cited. The work cannot be changed in any way or used commercially without permission from the journal.

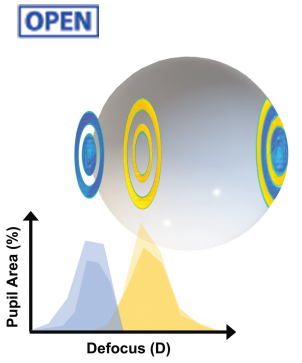

Author Affiliations:
[1]School of Optometry, Indiana University Bloomington, Bloomington, Indiana
[2]School of Optometry, Aston University, Birmingham, United Kingdom
[3]CooperVision Inc., Pleasanton, California
*viswa.ramasubramanian@gmail.com

In response to the high prevalence of myopia in young adults,[1] approaching 100% in certain demographics,[2,3] research efforts have sought to slow or stop the accelerated growth of young eyes.[4] A longer eye is associated with sight-threatening retinal pathologies[5–8] in later years. Most extant methods at the time of writing use various optical strategies to alter the retinal image in progressing myopic eyes.[9–12] Spectacle lenses containing central clear zones surrounded by either groups of plus powered small lenslets[10,13,14] or arrays of scatter sources[15] have demonstrated some efficacy at slowing myopia progression. Repurposed presbyopic multifocal contact lens designs[9,16,17] have generally proven less effective than a novel dual-focus contact lens[11] specifically designed for myopia control, which received U.S. Food and Drug Administration approval in the United States in 2019.[18] MiSight 1 Day (omafilcon A; CooperVision, San Ramon, CA; coopervision.com) soft (hydrophilic) contact lenses with dual-focus optics were approved by the U.S. Food and Drug Administration for daily wear and are indicated for the correction of myopic ametropia and for slowing the progression of myopia in children with nondiseased eyes, who at the initiation of treatment are 8 to 12 years of age and have a refraction of –0.75 to –4.00 D (spherical equivalent) with ≤0.75 D of astigmatism. The lens is to be discarded after each removal.

One type of myopia control intervention includes optical features designed to focus some proportion (e.g., 25 to 50%) of the light anterior to the retina. The resulting myopic defocus has been shown to attenuate or prevent the eye elongation induced by simultaneously present hyperopic defocus in model work.[19,20] Published data show that the small lenslets included in the Defocus Incorporated Multiple Segments spectacle lenses (MiYOSMART; Hoya Vision Care, Tokyo, Japan) have approximately +3.50 D of added power,[10,13] whereas the dual-focus contact lens (MiSight 1 Day) includes annular zones containing approximately +2.00 D of added power.[21] Missing from these descriptions of the lenses themselves is a quantification of the myopic defocus dose delivered to the myopic child's retina. This distinction is important because the ability for a myopia control intervention to deliver myopic defocus depends on the eye's optics and the lens' treatment zone design. Said another way, just because a lens has a zone or zones of +2.00 or +3.50 D, this does not mean this is the amount of myopic defocus that is introduced by the lenses when worn. Two key

Downloaded from http://journals.lww.com/optvissci by BhDMf5ePHKav1zEoum1tQfN4a+kJLhEZgbsIHo4XMi0hCywCX1AWnYQp/IlQrHD3i3D0OdRyi7TvSFl4Cf3VC4/OAVpDDa8KKGKV0Ymy+78= on 07/25/2023

parameters of the eye's optics will dominate the resultant defocus present at the retina. First and most significant is the accommodative response,[22] which is known to lag at near in most eyes and can lag more in some eyes than others,[21] potentially being larger in myopic eyes.[23,24] Accommodative lags will generate hyperopic defocus in the retinal image. Increased lags in myopic eyes wearing multifocal contact lenses have been reported,[25] which can become amplified after sustained use of the multifocal lenses.[16] Also, negative spherical aberration found in accommodating eyes[26–28] generates a hyperopic shift in refractive error with increasing distance from the pupil center.[29] For example, young accommodating eyes may have sufficient negative spherical aberration to counteract positive spherical aberration introduced in a contact lens,[30] which may explain the low impact of presbyopic contact lens designs when implemented as myopia control therapy.[16]

Model work has shown that the magnitude of introduced defocus will regulate eye growth[31–33] and the proportion of defocused light introduced to the retina.[34] Also, in the presence of a grow signal, studies have shown that more diopters of plus defocus[35] and a greater proportion of myopically defocused light[20,36] can both amplify the slowing effect of this optical treatment strategy. The present article sought to quantify the myopic defocus dose delivered and the associated reduction in hyperopically defocused light by the treatment optics of a dual-focus contact lens to the retina of children undergoing myopia control therapy.

Because the treatment optics of this contact lens are restricted to two narrow annuli, assessing the refractive impact of such lens designs with instruments that integrate over some device-determined region of the pupil cannot capture the zone-specific refractive impact.[37,38] Spatially resolved aberrometers, however, are ideally suited for this task in that they measure wavefront slope at many hundreds of locations in the pupil from which local refractive states can be calculated.[13] Introduced myopic defocus and reduced hyperopic defocus produced by the treatment optics can be quantified by assessing the refractive state in the geographic regions of the pupil covered by the treatment optic. Examining the full pupil, the same aberrometry data can be used to quantify increases in the proportion of myopically defocused light and decreases in the proportion of hyperopically defocused light in the retinal image.[31,32,34] Because of the success of the dual-focus contact lenses in slowing rate of myopia progression,[11,39,40] it was hypothesized that the dual-focus contact lens can consistently (*a*) deliver a significant dose of myopic defocus over a wide range of viewing distances in the eyes of treated myopic children and (*b*) decrease the amount of hyperopically defocused light in the retinal image.

METHODS

Subjects

Seventeen adolescent children aged 14 to 18 years (mean standard deviation [SD] age, 16.61 [1.63] years) and having completed either 3 or 6 years of myopia control therapy[40] with dual-focus soft contact lenses (MiSight 1 Day) were tested at the Aston University (United Kingdom) research clinic during their final year of treatment. This research was reviewed by the Aston University Research Ethics board and conforms with the principles and applicable guidelines for the protection of human subjects in biomedical research. Written informed consent or assent occurred with each participant as age-appropriate (and guardian consent where applicable) before entering in the aberrometry substudy. During the test visit, optical measurements were acquired from the right eye while children wore their dual-focus treatment lenses in both eyes. Subsequently, children wore matched power single-vision lenses (Proclear 1 Day; CooperVision) of the same distance prescription in both eyes with approximately 15 minutes of adaptation period before optical measurements of their right eyes. All participants were experienced and well-adapted contact lens wearers. No adaptation problems were reported. As previously published,[11] distance visual acuity was similar with both single-vision and dual-focus contact lenses. This study design allowed direct comparison of the optical impact of dual-focus and single-vision lenses on the central retinal images of right eyes while binocularly viewing stimuli over a wide range of distances. Both lenses shared the same base curve (8.7 mm), diameter (14.2 mm), and material (omafilcon A). The single-vision lenses use an aspherical front surface to avoid power variations in spherical aberration,[41] and the dual-focus lenses use a four-zone concentric design[42] with two zones (center zone and ring 2 [R2]) designed to correct the refractive myopia and two annular zones (ring 1 [R1] and ring 3 [R3]) identified as treatment zones with added plus power to generate myopic defocus at the retina. Eyes were fitted with lenses to optimize distance visual acuity using a maximum plus refraction technique.

Ex Vivo Contact Lens Aberrometry

Maps of optical power (Figs. 1A, B) across two sample –1.00 D lenses (single-vision and dual-focus) were measured *ex vivo* using a previously validated[43] single-pass Shack-Hartmann aberrometer (ClearWave; Lumetrics, Inc., Rochester, NY) with a sampling resolution of 104 μm. Distributions of sampled power (Fig. 1D) were plotted for each refractive correction zone (center zone and R2 of the dual-focus lens) and the two treatment zones (R1 and R3 of the dual-focus lens). To allow direct comparison between the two lenses, the same calculations were performed for the single-vision lens using identical regions of the measured wavefront (Fig. 1C). Average powers in the center zone of both lenses were within 0.02 D of the labeled –1.00 D power. The average added powers in the two treatment zones of the dual-focus lens were +2.00 and +2.25 D for R1 and R3, respectively. The increase in plus power within R3 is consistent with a small amount of positive spherical aberration. Conversely, the outer analysis zones of the single-vision lens have more negative power because of negative spherical aberration in this lens.[41]

Optical Measurements

A validated[44] double-pass pyramidal wavefront sensor (Osiris; CSO, Florence, Italy) was used to measure (sampling resolution of 41 μm) the wavefront exiting the right eye as children binocularly accommodated to high-contrast stimuli at distances of 3.98, 0.98, 0.48, 0.31, and 0.23 m (target vergence [D], of –0.25, –1.02, –2.08, –3.23, and –4.35 D). At 3.98 m, children viewed the 0.30 logMAR line on an illuminated Early Treatment Diabetic Retinopathy Study chart. At near viewing distances, the stimuli were changing sequences of high-contrast letters (0.30 logMAR equivalent) displayed on an iPhone 6 (Apple, Cupertino, CA) with the screen luminance of 150 cd/m^2. Room illumination during measurements was 6 lux. Head position was stabilized with both chin and forehead rests. The instrument measurement axis was aligned with the eye's primary line of sight. Therefore, when children accommodated binocularly to near stimuli, the left eye converged to maintain fixation, whereas the relative position of the right remained approximately constant throughout the experiment.

Downloaded from http://journals.lww.com/optvissci by BhDMf5ePHKav1zEoum1tQfN4a+kJLhEZgbsIHo4XMi0hCywCX1AWnYQp/IlQrHD3i3D0OdRyi7TvSFl4Cf3VC4/OAVpDDa8KKGKV0Ymy+78= on 07/25/2023

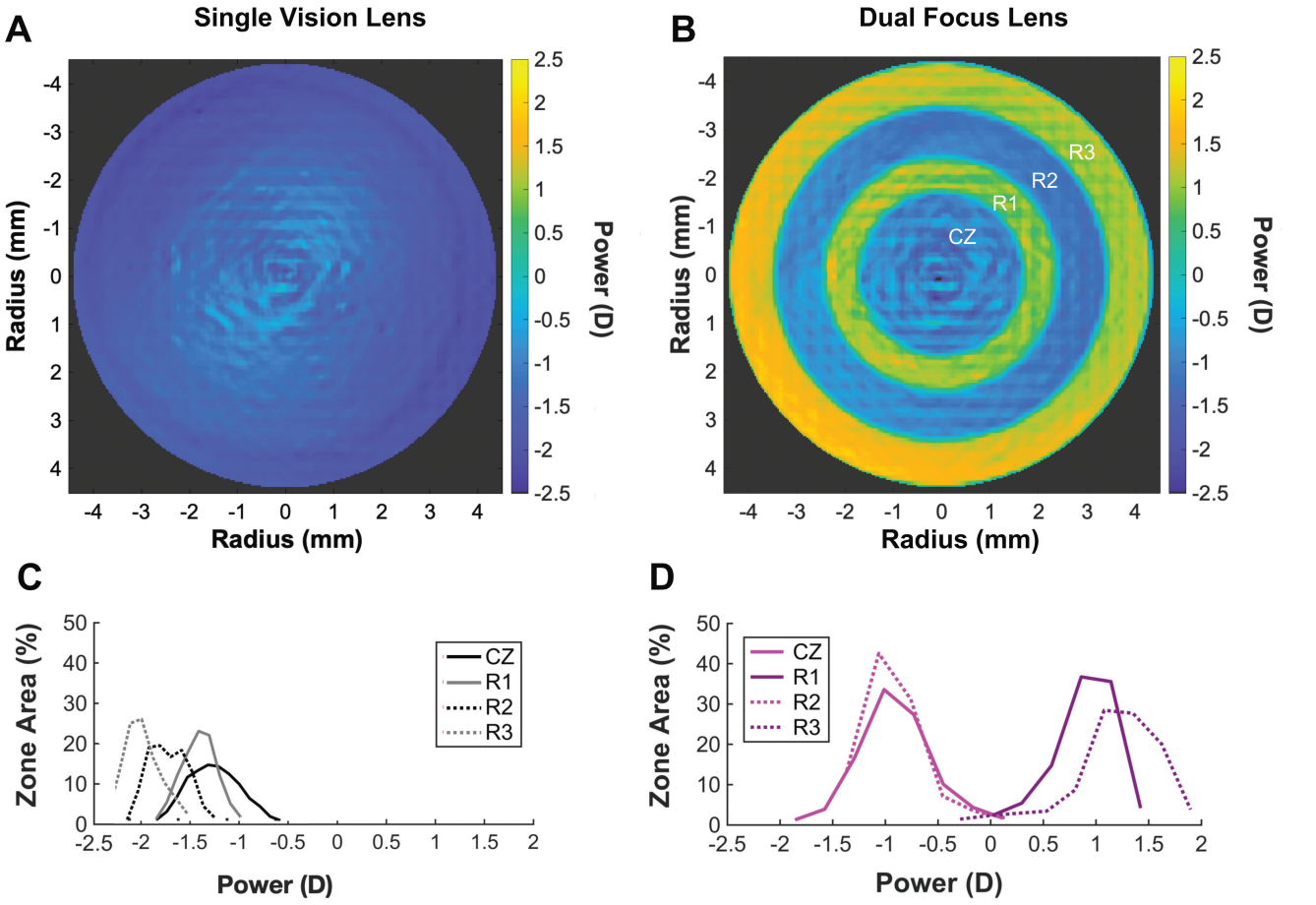

FIGURE 1. Off-eye optical design of the single-vision and dual-focus lenses. Measured (ClearWave; Lumetrics, lumetrics.com) power maps for two sample contact lenses (single-vision (A) and dual-focus (B)) with labeled power –1.00 D from which zone-specific power distributions (C, D) were derived. Rings on the single-vision power map (A) mirror the zone boundaries observed in the dual-focus lens (B). Power distributions (C, D) characterize each of the four zones, quantified using bin widths of 0.25 D.

Before each measurement, children were instructed to blink twice and keep the letters as clear as they could. Three repeats of good quality data were acquired at each stimuli position.

Data Analysis

Osiris wavefront error maps were imported into MATLAB (MathWorks, Natick, MA), and custom software (Indiana Wavefront Analyzer; MAPLE, Bloomington, IN) was used to compute local measures of refractive state in the pupil (natural pupil size) using the slope/radial distance equation.[38] The coordinate center was aligned with the contact lens center. Corrected refractive state maps were subdivided into geometric zones that matched the measured geometry of the dual-focus contact lens allowing a zone-specific assessment of the refractive impact of the dual-focus lenses. Data sets corrupted because of blinks, eye lashes, tear breakup, and momentary lapses of gaze and/or accommodation were manually excluded. Data cleaning used thresholding (exclude values <5% of the mode) and removal of local samples corrupted at pupil margins. Refractive states from cleaned data repeats were used to plot pooled refractive state histograms with bin width of 0.25 D for both dual-focus and single-vision lenses. In Fig. 2, the "repeat 1" data contain 29,422 measures of refractive states in the pupil (center zone, 5660; R1, 5623; R2, 11,213; and R3, 6926). Therefore, when three repeat measurements are pooled, the histograms reveal the distribution of approximately 88,266 refractive states (center zone, 16,980; R1, 16,869; R2, 33,639; and R3, 20,778) sampled across the pupil. The data processing sequence is shown with examples in Fig. 2.

From the pooled refractive state histograms, corresponding target vergence (–1/target distance in meters) was subtracted to yield pooled defocus histograms. Defocus (refractive state – target vergence) histograms across the full pupil were weighted by the Stiles-Crawford effect (σ = 0.115)[45] and were used to quantify the proportion of hyperopic (positive) and myopic (negative) defocus and focused light present at the retina. Pooled defocus values from each histogram were used to compute the mean and SD defocus contributed by each zone.

Stiles-Crawford effect weighted area of full pupil that produced myopically and hyperopically defocused light was used to quantify the proportion of myopically and hyperopically defocused light within the retinal image. Two sets of criteria were used to define myopic, hyperopic, and focused light. The first analysis used the common clinical thresholds[46,47] for defining myopia and hyperopia (refractive state values beyond –0.50 and +0.75 D), and a second pair of refractive criteria was based on the familiar depth of focus (±0.25 D) to define focused light (Fig. 3A). The resulting three

Downloaded from http://journals.lww.com/optvissci by BhDMf5ePHKav1zEoum1tQfN4a+kJLhEZgbsIHo4XMi0hCywCX1AWnYQp/IlQrHD3i3D0OdRyi7TvSFl4Cf3VC4/OAVpDDa8KKGKV0Ymy+78= on 07/25/2023

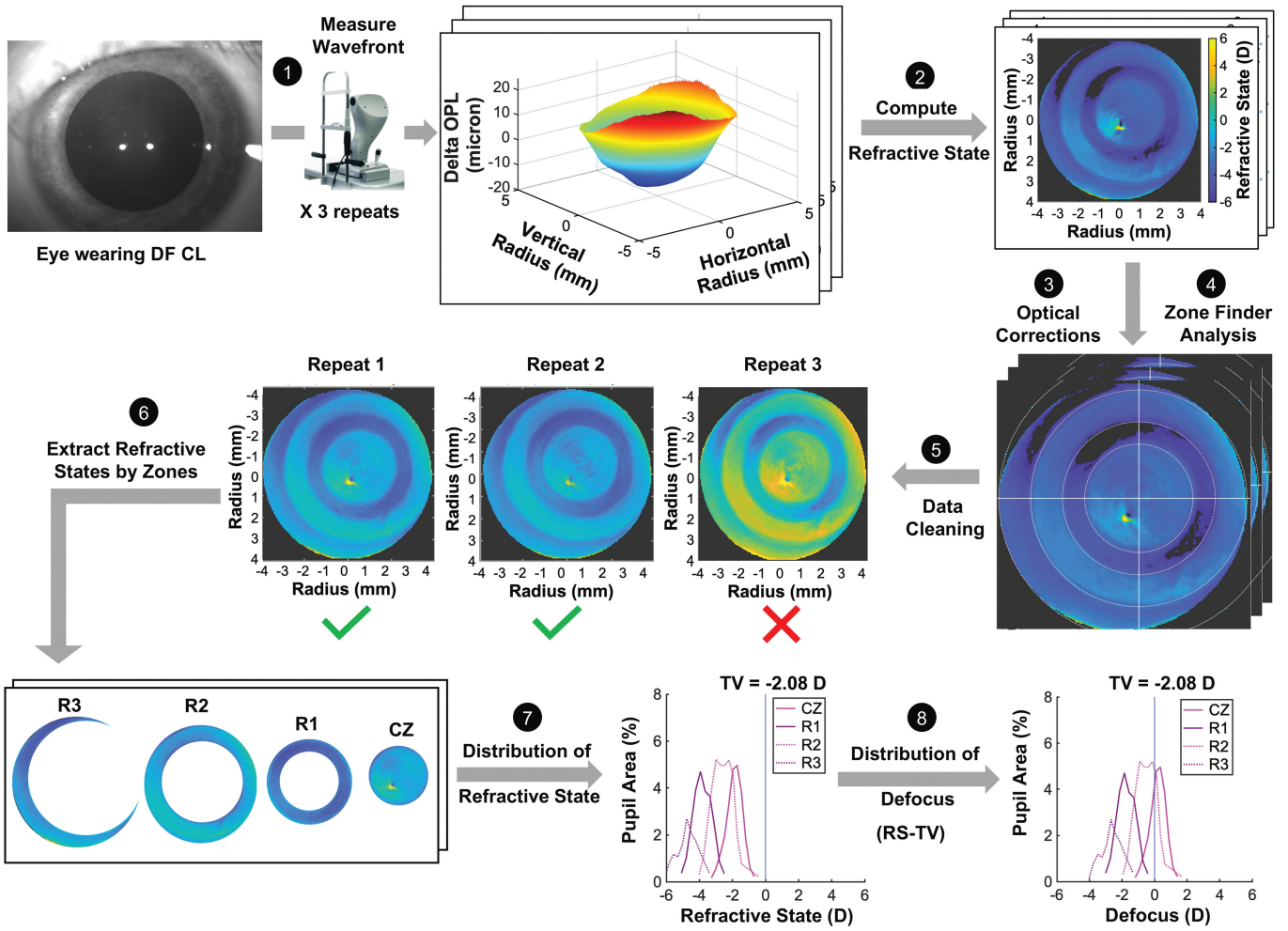

FIGURE 2. Data processing sequence with sample data starting at top left and finishing bottom right. (1) A sample anterior eye image collected from the aberrometer of an eye fit with a dual-focus CL, measured three times with the clinical Osiris aberrometer, which output three wavefront error maps. (2) Custom software implemented in MATLAB,[13] calculated the local refractive state for each sample in the wavefront revealing the expected four-annular-zone structure of the MiSight CL.[11] (3) Raw refractive state data were corrected for prism and lens centration errors, and (4) the measured zone geometry of this lens was used to locate zone boundaries in the maps. (5) In a few cases (3 of 17), it was observed that children would accommodate accurately on two of the three trials but fail to accommodate on the third. Mean data excluded the outlier data set. Also, data corrupted by blinks, lashes, and tear disruptions were excluded. (6) Refractive data from each zone (center zone and three surrounding rings, R1, R2, and R3) were isolated and (7) used to plot refractive state distributions for each individual zone. (8) Refractive state distributions were converted to defocus distributions by subtracting the target vergence (in diopters). CL = contact lens.

proportions (myopically and hyperopically defocused light and focused light) were plotted using three-axes ternary plots,[48] which revealed the proportion of each type of defocus by the position of a datum along all three axes of this triangular space. The defocus proportions are revealed by tracing each of the three colored lines that pass through a data point to the matched colored scale. The example in Fig. 3B shows a data point representing proportions of 0.3 myopic (red), 0.4 hyperopic (blue), and 0.3 focused (black) light.

RESULTS

To quantify the retinal defocus generated by each contact lens zone, the target vergence was subtracted from the measured refractive state, revealing the presence of myopically (negative valued) and hyperopically (positive valued) defocused light. On-eye defocus distributions are plotted for the full pupil (Fig. 4) and for each zone (Fig. 5, center zone, R1, R2, and R3) of a sample eye (18-year-old with a refractive error of –4.50 D in the right eye) fit with either a single-vision (top panels) or a dual-focus (bottom panels) lens for all five viewing distances (target vergences [D] of –0.25, –1.02, –2.08, –3.23, and –4.35 D). The height of each distribution at zero on the *x* axis indicated the percentage of focused light.

Center zone defocus distributions (Fig. 5) provided an indication of the accommodation accuracy, revealing low levels of myopic defocus when viewing a distant target (accommodative lead) and a gradual drift to hyperopic defocus as the target approached the eye (accommodative lag). With the single-vision lens, hyperopic defocus dominated the image generated by the two outer zones being greatest in R3, especially when the eye was accommodating (e.g., mode for R3 with –4.35 D target = +2 D). Similar trends were seen in the distance correction zone data from the same eye fit with the dual-focus lens

Downloaded from http://journals.lww.com/optvissci by BhDMf5ePHKav1zEoum1tQfN4a+kJLhEZgbsIHo4XMi0hCywCX1AWnYQp/IlQrHD3i3D0OdRyi7TvSFl4Cf3VC4/OAVpDDa8KKGKV0Ymy+78= on 07/25/2023

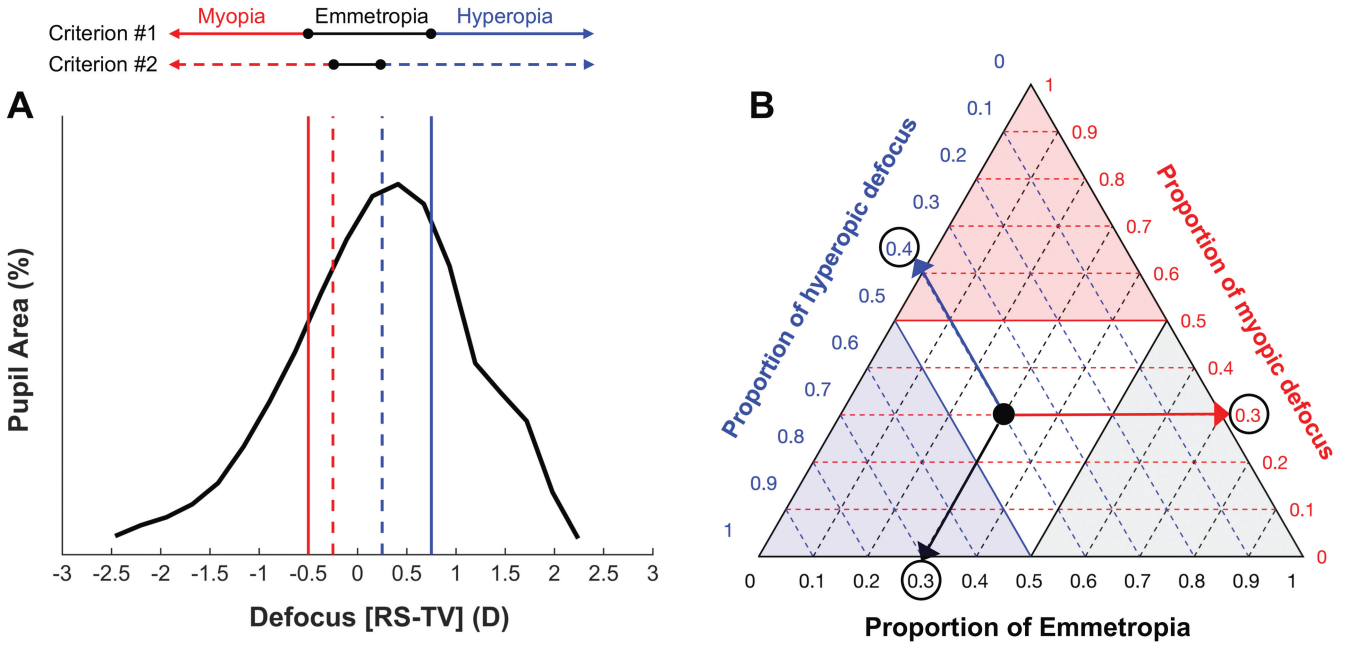

FIGURE 3. Methods used to classify the focused and defocused light in the retinal image. (A) Criteria for classifying myopically (red) and hyperopically (blue) defocused light and focused (black) light from the continuous distributions of measured retinal defocus. (B) Example ternary plot of the three dimensions of proportions of myopic, hyperopic, and focused light (red, blue, and black). Colored arrows show how proportions are determined for a given data point. Defocus = Refractive state (RS) – Target vergence (TV).

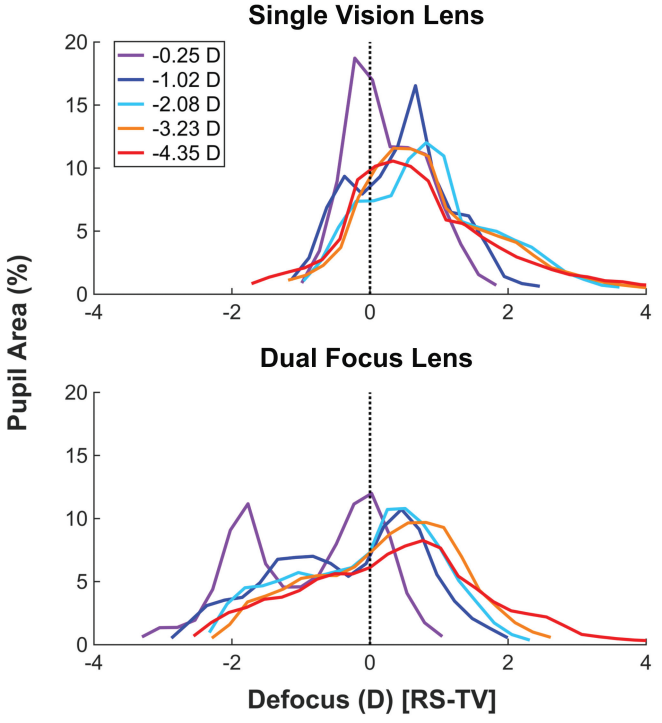

FIGURE 4. Full pupil defocus distributions from a sample eye. Defocus distributions (0.25 D bins) from the sample eye fit with the single-vision (top panel) and dual-focus (bottom panel) lenses for the full pupil. The measured refractive states were converted to defocus distributions (difference between the measured refractive state and the target vergence: defocus (diopters) = refractive state – target vergence) with positive values indicating hyperopically defocused light and negative for myopic defocus. Black dashed lines plot the position of the eye's retina where defocus is zero.

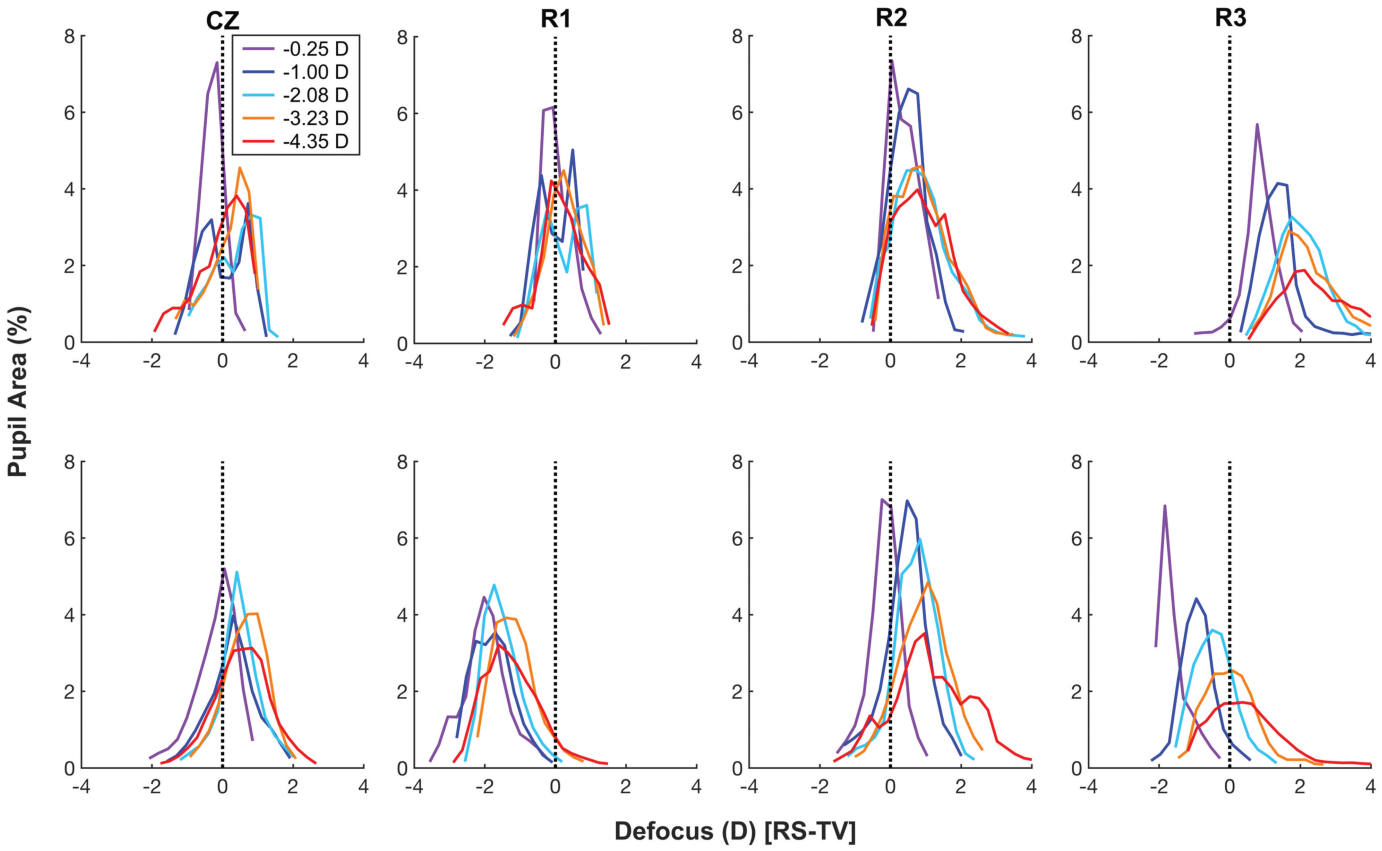

FIGURE 5. Zone-wise defocus distributions with single-vision and dual-focus lenses. Defocus distributions (0.25 D bins) for the same eye as Fig. 4, for four individual zones (two correction zones [center zone and R2] and two treatment zones [R1 and R3] for all five viewing distances). Defocus = Refractive state (RS) – Target vergence (TV).

(lower panels, center zone and R2), but the treatment zones (R1 and R3) revealed an obvious shift toward myopic defocus at all viewing distances, with defocus in R1 being almost exclusively myopic. The myopic shift observed in treatment R3 when viewing the 3.98 m target gradually shifted toward zero and included some hyperopic defocus at the nearest viewing distances (31 and 23 cm), reflecting the combined effects of accommodative lag and increased negative spherical aberration present in this young eye viewing near targets. The clear double-peaked defocus distributions created by the dual-focus lens seen in the full pupil data (Fig. 4) at the farther viewing distances (3.98 m and 98 cm) disappeared as spherical aberration levels increase with accommodation. For each lens and zone, as the target approached, the eye accommodated and the defocus distributions widened, revealing increased aberrations in this young accommodating eye. For example, the SD of the distributions for the full pupil increased from 0.81 to 1.56 D for the single-vision lens and from 1.23 to 1.54 D for the dual-focus lens, as the target approached from 3.98 m to 23 cm.

The mean defocus values from each of the four zones are plotted in Fig. 6 for each child (gray lines) and the sample mean (bold lines and symbols). Although the retinal images of individual children included slightly different levels of defocus, the central trends dominated, resulting in standard error of the mean (shown as error bars) values on the scale of the plotted symbols (average standard error of the mean, 0.20 D). The accommodative behavior of these children can be seen by examining the center zone data (Figs. 6A, B). With both single-vision and dual-focus lenses, children generally experienced small accommodative leads at distance (mean, –0.86 D for single-vision and –0.94 D for dual-focus), which transitioned to accommodative lag at near (mean, +0.59 D for single-vision and +0.98 D for dual-focus). Notably, these center zone data were almost identical for the single-vision and dual-focus lenses (mean difference, 0.14 D across all viewing distances), revealing that introduction of treatment optic zones (R1 and R3) in the dual-focus lenses did not affect the accommodative behavior. When comparing the pupil regions covered by the treatment zones (R1 and R3), defocus was consistently more myopic (R1 [dual-focus – single-vision] = –2.05 D, R3 [dual-focus – single-vision] = –2.40 D) when eyes were fit the dual-focus lens (Figs. 6C, D, G, H). The accommodative lag observed at near in the center zone data (Figs. 6A, B) steadily increased as measured farther from pupil center (R3 > R2 and R1), resulting in hyperopic defocus in eyes fit with single-vision lenses at nearest distances (mean defocus for targets 0.33 m and nearer; R1, 0.88 D; R2, 1.27 D; and R3, 1.70 D). This larger hyperopic shift at the pupil margins was caused by the well-documented increase in negative spherical aberration as the eye accommodates.[27,30] The combined accommodative lag and negative spherical aberration reduce the level of myopic defocus introduced by the treatment optics of the dual-focus lens. For example, R1 and R3 introduced –2.92 and –2.87 D of myopic defocus, respectively, at 4 m, which reduced to –0.63 and –0.27 D at 0.23 m. For stimuli beyond 0.4 m, all children experienced myopic defocus. For stimuli 0.31 m and nearer, 12 (71%) and 10 children (59%) experienced average myopic defocus in the pupil covered by R1 and R3 treatment zones, respectively.

Downloaded from http://journals.lww.com/optvissci by BhDMf5ePHKav1zEoum1tQfN4a+kJLhEZgbsIHo4XMi0hCywCX1AWnYQp/IlQrHD3i3D0OdRyi7TvSFl4Cf3VC4/OAVpDDa8KKGKV0Ymy+78= on 07/25/2023

Downloaded from http://journals.lww.com/optvissci by BhDMf5ePHKav1zEoum1tQfN4a+kJLhEZgbsIHo4XMi0hCywCX1AWnYQp/IlQrHD3i3D0OdRyi7TvSFl4Cf3VC4/OAVpDDa8KKGKV0Ymy+78= on 07/25/2023

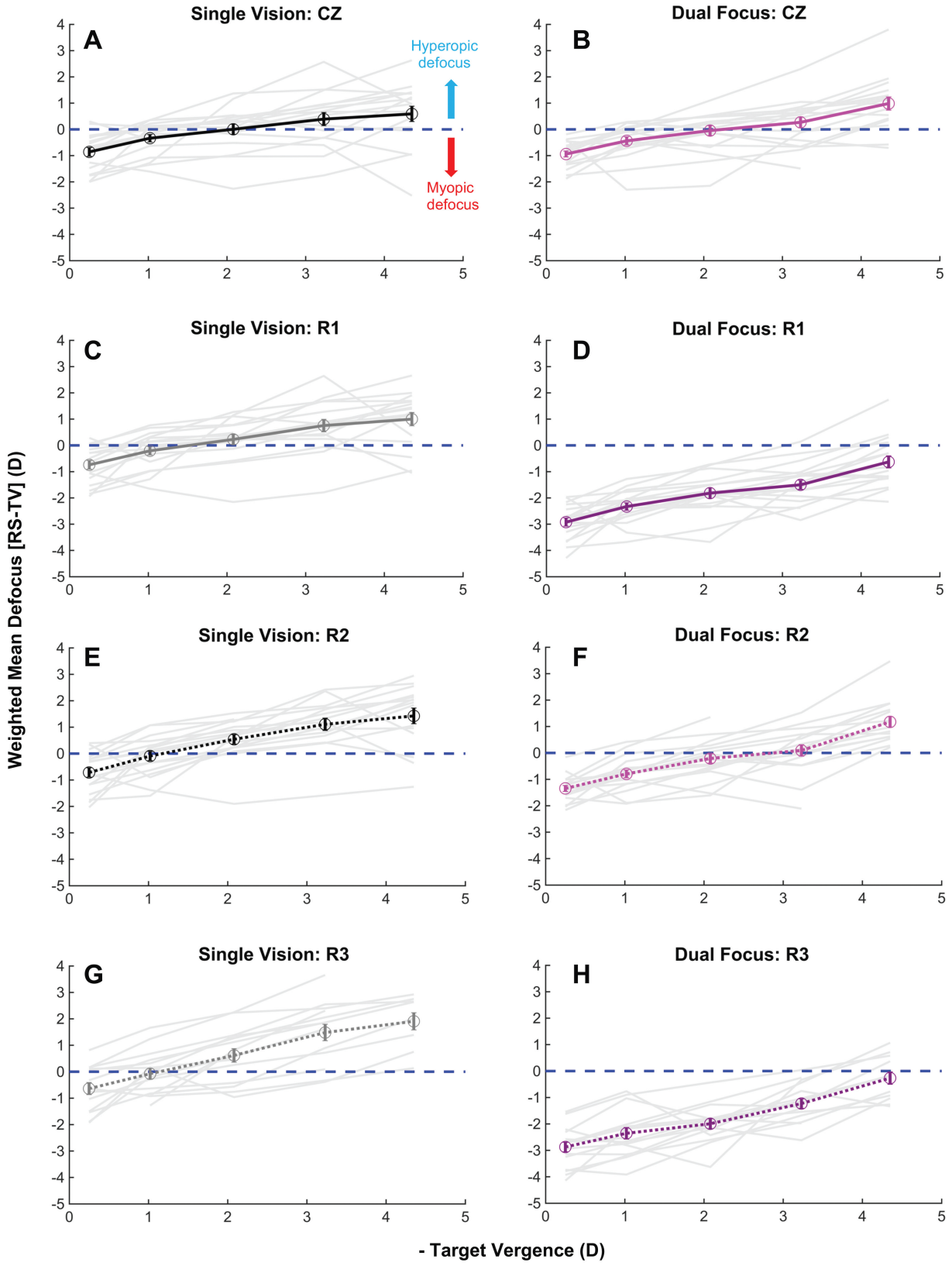

FIGURE 6. Mean defocus (defocus = refractive state – target vergence) as a function of target vergence from all children. Mean defocus values (*y* axis) observed at each target vergence (*x* axis) were plotted for each zone (center zone, R1, R2, and R3) for eyes fit with the single-vision (A, C, E, G) or the dual-focus (B, D, F, H) contact lenses. Data for each of the 17 tested eyes were plotted as gray lines, and the mean of the 17 was plotted as a bold line and symbol. Error bars were ±1 SEM. SEM = standard error of the mean.

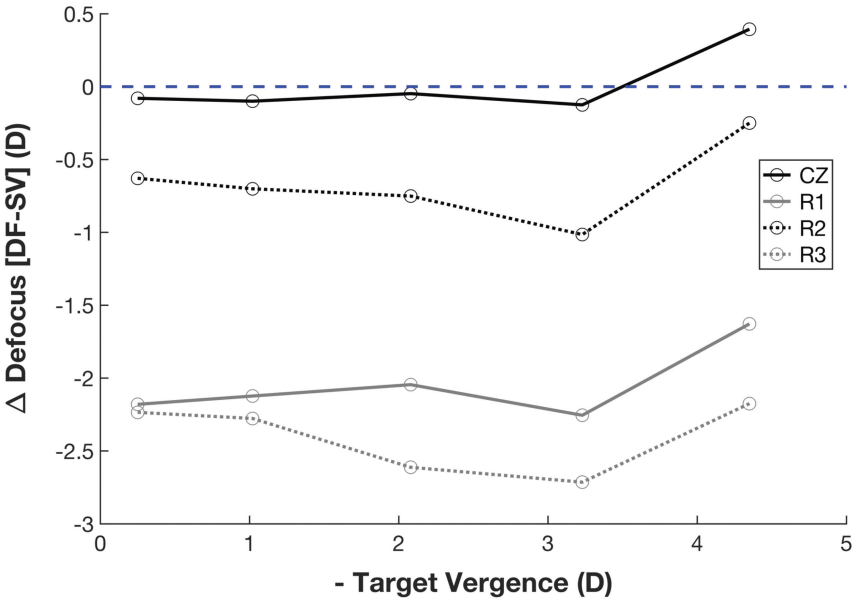

FIGURE 7. Zone-wise impact of dual-focus lens on the defocus of eyes compared with the single-vision control lens. Mean difference in defocus between the dual-focus and single-vision lens for four individual zones (two correction zones [center zone and R2] and two treatment zones [R1 and R3]) as a function of target vergence in diopters.

The impact of the treatment zones can be quantified by comparing the defocus generated by those regions of the pupil when fit with the dual-focus with the same regions of the pupil when the eye was fit with the single-vision lens. The difference in defocus between the dual-focus and single-vision lens for each zone is plotted in Fig. 7. The center correction zone generated the same levels of defocus (mean, 0.01 D), whereas, in the second correction zone (R2), on average, there was myopic defocus (mean, –0.66 D). However, when comparing regions of the pupil covered by the treatment optics (R1 and R3), the dual-focus lens created, on average, a –2.05-D myopic shift in defocus for R1 and a –2.40-D shift for R3, which varied little with viewing distance. The data in Figs. 6 and 7 show the ability of the dual-focus lens to achieve two goals, generating significant myopic defocus across the full pupil at the greater viewing distances (mean, –2.25 D between 3.98 and 0.48 m) and a combined introduction of myopic defocus (–0.91 D for distances ≤0.31 m) and removal of the significant hyperopic defocus observed in eyes fit with the single-vision lens when viewing near stimuli (mean, 1.29 D for distances ≤0.31 m).

The aforementioned analysis of the data in Figs. 6 and 7 characterizes the myopia control dose delivered by each treatment optic in units of diopters. However, it has been shown in model work[20] that the amount of myopically defocused light on the retina plays a significant role in influencing eye growth. Therefore, the next section focuses on the proportion of the light forming the retinal image, which can be considered to contribute to myopia control (increase in the proportion of myopically defocused light and reduction in the proportions of hyperopically defocused light). Central to this analysis is the underlying geometry of the dual-focus lens (Fig. 2) and the proportion of the pupil covered by each of its zones. The average percentages of the full pupil covered by each of the four zones remained relatively stable across all viewing distances because pupil size varied little with viewing distance (e.g., mean diameter was 6.57 mm when viewing a distance target and 6.34 mm when viewing a near target at 0.23 m).

Using the refractive criteria shown in Fig. 3A, the three proportions of focused and myopically and hyperopically defocused light extracted from the full pupil defocus distributions of each eye and each lens were depicted graphically in ternary plots for eyes fit with both the single-vision (Figs. 8A, C) and dual-focus (Figs. 8B, D) lenses for all viewing distances tested: 3.98 m (filled circles), 0.98 m (open circles), 0.48 m (open squares), 0.31 m (open diamonds), and 0.23 m (filled triangles). Predictably, the criterion set with the wider range for defining "focused" (–0.50 to +0.75 D) generated larger proportions of focused light (Figs. 8A, B) than the data using the narrow range (±0.25 D) plotted in Figs. 8C and D. In every case, there was a consistent drift in the data from the upper regions (red shaded) indicating retinal images dominated by myopic defocus to the lower left blue region where images were dominated by hyperopic defocus. For example, while viewing the farthest target, approximately 62 (single-vision) and 87% (dual-focus) of the full pupil was dominated by myopic defocus, which reduced to 18 (single-vision) and 27% (dual-focus) for the nearest target. Conversely, the proportion of hyperopic defocus in the retinal image increased from 10 (single-vision) and 3 (dual-focus) to 69 (single-vision) and 50% (dual-focus) for the farthest and nearest viewing distances, respectively. The bias toward myopic defocus and away from hyperopic defocus created by the dual-focus lens can be observed by comparing the locations of corresponding data in the right and left panels of Fig. 8. Although it is convenient to quantify the proportions (or percentage) of the pupil generating each type of defocus, these percent values will vary with pupil size, as shown for other lens designs with radially varying power.[49]

The treatment dose introduced by the R1 and R3 zones of the dual-focus lens can be quantified as the increase in proportion of myopically defocused light and the decrease in proportion of hyperopically defocused light in the retinal image created by the dual-focus optic; each occurs simultaneously at each viewing distance. These shifts in the proportion of myopically defocused and hyperopically defocused light were quantified and are shown in

Downloaded from http://journals.lww.com/optvissci by BhDMf5ePHKav1zEoum1tQfN4a+kJLhEZgbsIHo4XMi0hCywCX1AWnYQp/IlQrHD3i3D0OdRyi7TvSFl4Cf3VC4/OAVpDDa8KKGKV0Ymy+78= on 07/25/2023

Downloaded from http://journals.lww.com/optvissci by BhDMf5ePHKav1zEoum1tQfN4a+kJLhEZgbsIHo4XMi0hCywCX1AWnYQp/IlQrHD3i3D0OdRyi7TvSFl4Cf3VC4/OAVpDDa8KKGKV0Ymy+78= on 07/25/2023

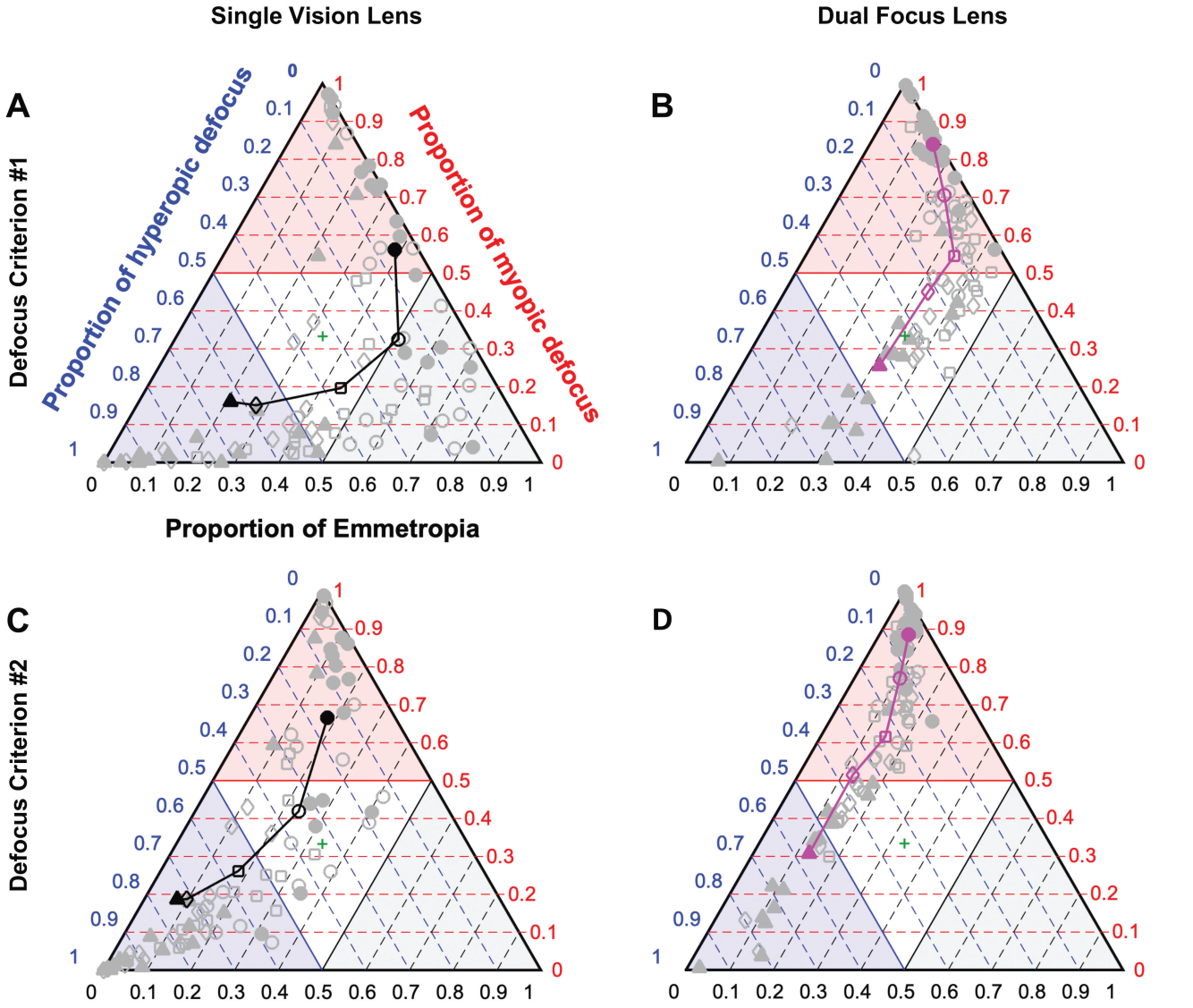

FIGURE 8. Ternary plots of focused and defocused light in the retinal image. The three proportions of focused and myopically and hyperopically defocused light forming the foveal images were extracted from the full pupil defocus distributions (Fig. 4) and plotted for each eye and each lens using three axes ternary plots. Data for eyes fit with the single-vision (A, C) and dual-focus (B, D) lenses for each viewing distance: 3.98 (filled circles), 0.98 (open circles), 0.48 (open squares), 0.31 (open diamonds), and 0.23 m (filled triangles) are plotted for the sample means (bold symbols and lines) and for each eye (low contrast gray symbols).

Table 1. Introduction of additional myopically defocused light (between 30 and 40%) dominated at the larger viewing distances, whereas reduction in the proportion of hyperopically defocused light dominated at the nearest distances. Despite the added plus power in the treatment rings, the dual-focus lens design was able to maintain similar proportion of focused light in the retinal image as the single-vision lens at each viewing distance (average, 20%).

DISCUSSION

The main purpose of this study was to quantify the myopia treatment dose delivered by a myopia control dual-focus contact lens containing two annular treatment zones, which include approximately 2.00 D of added plus power (Fig. 1). Dose was assessed along two dimensions: the diopters of defocus created in the retinal image (Figs. 4 to 7) and the proportion of myopically and hyperopically defocused light within these retinal images (Figs. 3, 8). The data summarized in this article show that, on both scales (diopters and proportion of light in the image), the dual-focus contact lens treatment optics successfully introduced an average myopia control dose of 2.00 D into the retinal image at all viewing distances. These results are consistent with the proposed closed-loop optical mechanisms by which dual-focus myopia-control contact[40] and spectacle[15] lenses achieve treatment success.

The similar defocus levels observed in pupil regions covered by the center zones (Figs. 6A, B) of both single-vision and dual-focus lenses reveal that the dual-focus optics did not disrupt normal

TABLE 1. Optical impact of dual-focus lens on the proportion of focused and defocused light in the retinal image relative to the single-vision control lens

Defocus criterion 1			
Target vergence (D)	Δ Proportion (%) of hyperopic defocus (DF-SV)	Δ Proportion (%) of myopic defocus (DF-SV)	Δ Proportion (%) of focused light (DF-SV)
–0.25	–0.04 (–4%)	0.28 (+28%)	–0.24 (–24%)
–1.02	–0.11 (–11%)	0.38 (+38%)	–0.27 (–27%)
–2.08	–0.25 (–25%)	0.35 (+35%)	–0.10 (–10%)
–3.23	–0.35 (–35%)	0.30 (+30%)	0.06 (+6%)
–4.35	–0.20 (–20%)	0.09 (+9%)	0.11 (+11%)
Defocus criterion 2			
Target vergence (D)	Δ Proportion (%) of hyperopic defocus (DF-SV)	Δ Proportion (%) of myopic defocus (DF-SV)	Δ Proportion (%) of focused light (DF-SV)
–0.25	–0.11 (–11%)	0.22 (+22%)	–0.11 (–11%)
–1.02	–0.22 (–22%)	0.35 (+35%)	–0.13 (–13%)
–2.08	–0.33 (–33%)	0.35 (+35%)	–0.03 (–3%)
–3.23	–0.35 (–35%)	0.33 (+33%)	0.03 (–3%)
–4.35	–0.17 (–17%)	0.12 (+12%)	0.05 (–5%)

Proportional changes in hyperopically defocused, myopically defocused, and focused light created by the dual-focus and the single-vision contact lenses for each target vergence and for the two refractive criteria used to segregate the defocus scale into three dimensions (proportions of focused and of myopically and hyperopically defocused light in the retinal image, see Fig. 3A). DF-SV = dual-focus–single-vision.

Downloaded from http://journals.lww.com/optvissci by BhDMf5ePHKav1zEoum1tQfN4a+kJLhEZgbsIHo4XMi0hCywCX1AWnYQp/IlQrHD3i3D0OdRyi7TvSFl4Cf3VC4/OAVpDDa8KKGKV0Ymy+78= on 07/25/2023

accommodation.[50] The leads and lags similarly contribute to the defocus levels created by the noncentral annular correction zone, but at the increased distance from the lens and pupil center of this annular zone, spherical aberrations of the contact lens and that of the eye also contribute to the resulting defocus patterns. The essentially normal accommodative behavior seen in eyes fit with the dual-focus lenses reveals that the correction zones (center zone and R2) remain the focus target for these eyes, with no evidence that children use the added plus power in the treatment zones to focus near targets. This result is crucial for such lenses to be able to deliver myopic defocus with the treatment optics.

As reported previously for adult eyes,[27,28] spherical aberration of the adolescent eyes in this study (mean age, 16.61 years) drifted negatively as the eye's lens changes shape during accommodation. Changes in spherical aberration of eyes fit with single-vision lenses were quantified with the Zernike coefficient C40 for wavefronts measured across the full pupil at each viewing distance. Average pupil diameters were 6.60, 7.05, 7.04, 6.85, and 6.34 mm for viewing distances of 3.98, 0.98, 0.48, 0.31, and 0.23 m, respectively. Although there were individual differences in absolute levels of spherical aberration, accommodation induced a negative shift in all eyes, resulting in a mean spherical aberration (eye + single-vision lens) that increased from –0.07 to –0.50 μm as the viewing distance was reduced from 3.98 to 0.23 m with a best fit slope of –0.105 μm per diopter of target vergence. Spherical aberration of eyes with dual-focus contact lens was not determined, as the Zernike polynomials cannot accurately fit the zonal power profile of this lens (Figs. 1B, D).

Because accommodation was unaffected by the dual-focus optics of the MiSight 1 Day lenses relative to single-vision lenses, ocular spherical aberration changes resulting from changing eye lens shape are matched for eyes fit with single-vision and dual-focus lenses. For this reason, the differences in average defocus of each zone between the single-vision and dual-focus lenses (Fig. 7) generally remained unchanged with target vergence. The resulting defocus differences, however, reflect radial differences in power of the two lenses. The added plus power in the dual-focus treatment zones created between –2.00 and –2.50 D of added myopic defocus and the negative spherical aberration of the single-vision lens resulted in the outer correction zone of eyes fit with the dual-focus lens (R2) being approximately –0.50 D more myopic. The increasing levels of negative spherical aberration observed in accommodating eyes resulted in increased hyperopic shifts that increased with radial distance from the pupil center (Fig. 6). The hyperopic shifts were small for distance viewing; for example, the mean shift in the outer correction ring R2 of the single-vision lens is less than 0.25 D for viewing distance of ≥1 m. However, at the closest distances, the hyperopic shifts can exceed 1.00 D at the edge of the pupils. These high levels of negative spherical aberration impact the defocus values associated with each zone.[49,51] For example, the hyperopic drift in defocus values (Fig. 6) associated with closer viewing distances (≤31 cm) is 0.49 D in the center zone of the single-vision, and this increases to 0.88 D for R1, 1.27 D for R2, and 1.70 D for R3. The extra 1.20 D of hyperopic shift observed in R3 compared with center zone is directly attributable to the changes in spherical aberration levels of the accommodating eyes.

The current study evaluated the real-world situation where contact lenses are nominally decentered on eye. The impact of contact lens movement during the interblink interval, however, was minimized with our blink-blink-capture protocol described in the methods, which, in most cases, resulted in three consistent repeat measures. Contact lens decentrations were small (0.37 mm temporally and 0.36 mm inferiorly) and had little or no effect on the proportion of light being imaged through the zones. For an average pupil size of 6.80 mm and average inferotemporal decentration of 0.37 mm, the changes in proportion of light imaged through the zones were as follows: center zone and R1, 0%; R2, –3.47%; and R3, +3.47%.

Downloaded from http://journals.lww.com/optvissci by BhDMf5ePHKav1zEoum1tQfN4a+kJLhEZgbsIHo4XMi0hCywCX1AWnYQp/IlQrHD3i3D0OdRyi7TvSFl4Cf3VC4/OAVpDDa8KKGKV0Ymy+78= on 07/25/2023

Quantifying the dose experienced in human children undergoing myopia control treatment is complicated because of the influence of accommodative responses, variability in pupil size (mean SD, 0.80 mm), and levels of negative spherical aberration. All three factors are expected to vary between individuals and to be significantly influenced by lifestyle and educational experiences, both of which have been implicated in the generation of myopia.[52,53] Increased outside playtime (with presumed longer viewing distances and smaller pupils) successfully lowered the incidence of myopia onset in a group of Asian children.[54] Restricting myopic defocus to peripheral lens locations, as will happen with a positive spherical aberration multifocal design (e.g., +0.175 μm of C40 over a 5-mm pupil diameter),[16] may fail to slow myopia progression either because pupil sizes are too small to include the required added plus power or because the significant negative spherical aberration of the children's eyes will inevitably reduce or even cancel the positive spherical aberration of a multifocal lens during near viewing.

As with all laboratory studies, this study captures a moment in time. However, by inference, the data provide information about the extended myopic control dosages experienced by young eyes as they are treated throughout the day and over multiple years. By using typical small text displayed on a high-resolution smartphone viewed binocularly, the goal was to capture data that are at some level reasonably representative of a good portion of a child's life. The singular defocus values captured from aberrometry measurements embrace monochromatic aberrations of the eye plus lens combination but, of course, fail to include the spread of defocus contributed by spectral changes in power of the human eye[55] and the effect of soft contact lens decentration on the anterior eye surface.

In conclusion, the data presented in this study reveal a consistent and universal increase in the nominal "stop" signal (more myopic defocus) and a simultaneous reduction in the hypothesized hyperopic defocus "grow" signal[56] in the central retina of children who were being treated with the dual-focus contact lenses. Although studies of infant monkeys have shown that hyperopic defocus outside of the central retina is sufficient to stimulate eye growth,[57] near viewing of small targets such as cell phones or books may only generate hyperopic defocus in and around the central retina, with the noncentral retina being more myopically defocused by virtue of being farther than the near target being viewed.[58]

ARTICLE INFORMATION

Submitted: September 29, 2022

Accepted: April 1, 2023

Funding/Support: None of the authors have reported funding/support.

Conflict of Interest Disclosure: NSL and PSK received financial support from CooperVision. MR is a consultant to CooperVision. PC, BA, and AB are employees of CooperVision. The sponsor participated in study design, analysis, and interpretation. All authors were responsible for the preparation of this article and the decision to submit this article for publication. The investigators at Aston University (NSL, SJ) had full access to the study data; the Indiana University investigators (VR, DM, MJ, MR, PSK) had partial access to the study data and take full responsibility for their presentation in this article. The lead author affirms that the article is an honest, accurate, and transparent account of the study being reported and that no important aspects of the study have been omitted. All investigators take responsibility for the integrity of the data and have critically reviewed the article for important intellectual content.

Author Contributions and Acknowledgments: Conceptualization: VR, NSL, DM, PC, BA, AB, PSK; Data Curation: VR; Formal Analysis: VR, DM, MJ, MR, PC, BA, AB, PSK; Investigation: VR, NSL, SJ, PC, BA, AB, PSK; Methodology: VR, DM, MJ, MR, PC, BA, AB, PSK; Project Administration: NSL, SJ, PC, BA, AB, PSK; Resources: NSL, SJ, AB, PSK; Software: VR, MJ, MR; Supervision: NSL, PC, BA, AB, PSK; Validation: VR; Visualization: VR, DM, AB, PSK; Writing – Original Draft: VR, AB; Writing – Review & Editing: VR, NSL, DM, MJ, MR, PC, BA, AB, PSK.

The authors thank the Clinical Optics Research Lab members for their useful insights on the data analysis.

REFERENCES

1. Holden BA, Fricke TR, Wilson DA, et al. Global Prevalence of Myopia and High Myopia and Temporal Trends from 2000 through 2050. Ophthalmology 2016;123:1036–42.

2. Ding BY, Shih YF, Lin LL, et al. Myopia among Schoolchildren in East Asia and Singapore. Surv Ophthalmol 2017;62:677–97.

3. Jung SK, Lee JH, Kakizaki H, et al. Prevalence of Myopia and Its Association with Body Stature and Educational Level in 19-year-old Male Conscripts in Seoul, South Korea. Invest Ophthalmol Vis Sci 2012;53:5579–83.

4. Wildsoet CF, Chia A, Cho P, et al. IMI — Interventions Myopia Institute: Interventions for Controlling Myopia Onset and Progression Report. Invest Ophthalmol Vis Sci 2019;60:M106–31.

5. Fricke TR, Jong M, Naidoo KS, et al. Global Prevalence of Visual Impairment Associated with Myopic Macular Degeneration and Temporal Trends from 2000 through 2050: Systematic Review, Meta-analysis and Modelling. Br J Ophthalmol 2018;102:855–62.

6. Klaver CC, Wolfs RC, Vingerling JR, et al. Age-specific Prevalence and Causes of Blindness and Visual Impairment in an Older Population: The Rotterdam Study. Arch Ophthalmol 1998;116:653–8.

7. Tang Y, Wang X, Wang J, et al. Prevalence and Causes of Visual Impairment in a Chinese Adult Population: The Taizhou Eye Study. Ophthalmology 2015;122:1480–8.

8. Xiao O, Guo X, Wang D, et al. Distribution and Severity of Myopic Maculopathy among Highly Myopic Eyes. Invest Ophthalmol Vis Sci 2018;59:4880–5.

9. Walline JJ, Walker MK, Mutti DO, et al. Effect of High Add Power, Medium Add Power, or Single-vision Contact Lenses on Myopia Progression in Children: The Blink Randomized Clinical Trial. JAMA 2020;324:571–80.

10. Lam CS, Tang WC, Qi H, et al. Effect of Defocus Incorporated Multiple Segments Spectacle Lens Wear on Visual Function in Myopic Chinese Children. Transl Vis Sci Technol 2020;9:11.

11. Chamberlain P, Peixoto-de-Matos SC, Logan NS, et al. A 3-year Randomized Clinical Trial of MiSight Lenses for Myopia Control. Optom Vis Sci 2019;96:556–67.

12. Smith EL, 3rd. Optical Treatment Strategies to Slow Myopia Progression: Effects of the Visual Extent of the Optical Treatment Zone. Exp Eye Res 2013;114:77–88.

13. Jaskulski M, Singh NK, Bradley A, et al. Optical and Imaging Properties of a Novel Multi-segment Spectacle Lens Designed to Slow Myopia Progression. Ophthalmic Physiol Opt 2020;40:549–56.

14. Bao J, Yang A, Huang Y, et al. One-year Myopia Control Efficacy of Spectacle Lenses with Aspherical Lenslets. Br J Ophthalmol 2022;106:1171–6.

15. Rappon J, Chung C, Young G, et al. Control of Myopia Using Diffusion Optics Spectacle Lenses: 12-Month Results of a Randomised Controlled, Efficacy and Safety Study (CYPRESS). Br J Ophthalmol 2022;bjophthalmol–2021–321005.

16. Cheng X, Xu J, Chehab K, et al. Soft Contact Lenses with Positive Spherical Aberration for Myopia Control. Optom Vis Sci 2016;93:353–66.

17. Berntsen DA, Sinnott LT, Mutti DO, et al. A Randomized Trial Using Progressive Addition Lenses to Evaluate Theories of Myopia Progression in Children with a High Lag of Accommodation. Invest Ophthalmol Vis Sci 2012;53:640–9.

18. U.S. Food and Drug Administration (FDA). MiSight 1 Day (omafilcon A) Soft (Hydrophilic) Contact Lenses for Daily Wear. Available at: https://www.accessdata.fda.gov/Scripts/Cdrh/Cfdocs/Cfpma/Pma.Cfm?Id=P180035. Accessed September 19, 2022.

19. Arumugam B, Hung LF, To CH, et al. The Effects of Simultaneous Dual Focus Lenses on Refractive Development in Infant Monkeys. Invest Ophthalmol Vis Sci 2014;55:7423–32.

20. Arumugam B, Hung LF, To CH, et al. The Effects of the Relative Strength of Simultaneous Competing Defocus Signals on Emmetropization in Infant Rhesus Monkeys. Invest Ophthalmol Vis Sci 2016;57:3949–60.

21. Singh NK, Meyer D, Jaskulski M, et al. Retinal Defocus in Myopes Wearing Dual-focus Zonal Contact Lenses. Ophthalmic Physiol Opt 2022;42:8–18.

Downloaded from http://journals.lww.com/optvissci by BhDMf5ePHKav1zEoum1tQfN4a+kJLhEZgbsIHo4XMi0hCywCX1AWnYQp/IlQrHD3i3D0OdRyi7TvSFl4Cf3VC4/OAVpDDa8KKGKV0Ymy+78= on 07/25/2023

22. Cheng X, Xu J, Brennan NA. Accommodation and Its Role in Myopia Progression and Control with Soft Contact Lenses. Ophthalmic Physiol Opt 2019;39:162–71.

23. Mutti DO, Mitchell GL, Hayes JR, et al. Accommodative Lag before and after the Onset of Myopia. Invest Ophthalmol Vis Sci 2006;47:837–46.

24. Nakatsuka C, Hasebe S, Nonaka F, et al. Accommodative Lag under Habitual Seeing Conditions: Comparison between Myopic and Emmetropic Children. Jpn J Ophthalmol 2005;49:189–94.

25. Tarrant J, Severson H, Wildsoet CF. Accommodation in Emmetropic and Myopic Young Adults Wearing Bifocal Soft Contact Lenses. Ophthalmic Physiol Opt 2008;28:62–72.

26. Cheng H, Barnett JK, Vilupuru AS, et al. A Population Study on Changes in Wave Aberrations with Accommodation. J Vis 2004;4:272–80.

27. Lopez-Gil N, Fernandez-Sanchez V. The Change of Spherical Aberration during Accommodation and Its Effect on the Accommodation Response. J Vis 2010;10:12.

28. Plainis S, Ginis HS, Pallikaris A. The Effect of Ocular Aberrations on Steady-state Errors of Accommodative Response. J Vis 2005;5:466–77.

29. Thibos LN, Bradley A, Lopez-Gil N. Modelling the Impact of Spherical Aberration on Accommodation. Ophthalmic Physiol Opt 2013;33:482–96.

30. Altoaimi BH, Almutairi MS, Kollbaum PS, et al. Accommodative Behavior of Young Eyes Wearing Multifocal Contact Lenses. Optom Vis Sci 2018;95:416–27.

31. Howlett MH, McFadden SA. Spectacle Lens Compensation in the Pigmented Guinea Pig. Vision Res 2009;49:219–27.

32. Troilo D, Totonelly K, Harb E. Imposed Anisometropia, Accommodation, and Regulation of Refractive State. Optom Vis Sci 2009;86:E31–9.

33. Smith EL, 3rd, Hung LF. The Role of Optical Defocus in Regulating Refractive Development in Infant Monkeys. Vision Res 1999;39:1415–35.

34. Winawer J, Wallman J. Temporal Constraints on Lens Compensation in Chicks. Vision Res 2002; 42:2651–68.

35. Tse DY, Lam CS, Guggenheim JA, et al. Simultaneous Defocus Integration during Refractive Development. Invest Ophthalmol Vis Sci 2007;48:5352–9.

36. McFadden SA, Tse DY, Bowrey HE, et al. Integration of Defocus by Dual Power Fresnel Lenses Inhibits Myopia in the Mammalian Eye. Invest Ophthalmol Vis Sci 2014;55:908–17.

37. Gifford KL, Schmid KL, Collins JM, et al. Multifocal Contact Lens Design, Not Addition Power, Affects Accommodation Responses in Young Adult Myopes. Ophthalmic Physiol Opt 2021;41:1346–54.

38. Altoaimi BH, Kollbaum P, Meyer D, et al. Experimental Investigation of Accommodation in Eyes Fit with Multifocal Contact Lenses Using a Clinical Auto-refractor. Ophthalmic Physiol Opt 2018;38:152–63.

39. Hammond D, Chamberlain P, Arumugam B, et al. Eye Growth of Children Undergoing Myopia Control Treatment Compared with Emmetropic Eye Growth. Ophthalmologe 2022;119:147–8.

40. Chamberlain P, Bradley A, Arumugam B, et al. Long-term Effect of Dual-focus Contact Lenses on Myopia Progression in Children: A 6-year Multicenter Clinical Trial. Optom Vis Sci 2022;99:204–12.

41. Kollbaum PS, Bradley A, Thibos LN. Comparing the Optical Properties of Soft Contact Lenses On and Off the Eye. Optom Vis Sci 2013;90:924–36.

42. Kollbaum PS, Jansen ME, Tan J, et al. Vision Performance with a Contact Lens Designed to Slow Myopia Progression. Optom Vis Sci 2013;90:205–14.

43. Kollbaum P, Jansen M, Thibos L, et al. Validation of an Off-eye Contact Lens Shack-Hartmann Wavefront Aberrometer. Optom Vis Sci 2008;85:E817–28.

44. Singh NK, Jaskulski M, Ramasubramanian V, et al. Validation of a Clinical Aberrometer Using Pyramidal Wavefront Sensing. Optom Vis Sci 2019;96:733–44.

45. Applegate RA, Lakshminarayanan V. Parametric Representation of Stiles-Crawford Functions: Normal Variation of Peak Location and Directionality. J Opt Soc Am (A) 1993;10:1611–23.

46. Flitcroft DI, He M, Jonas JB, et al. IMI—Defining and Classifying Myopia: A Proposed Set of Standards for Clinical and Epidemiologic Studies. Invest Ophthalmol Vis Sci 2019;60:M20–30.

47. Leat SJ. To Prescribe or Not to Prescribe? Guidelines for Spectacle Prescribing in Infants and Children. Clin Exp Optom 2011;94:514–27.

48. Howarth RJ. Sources for a History of the Ternary Diagram. Br J Hist Sci 1996;29:337–56.

49. Bradley A, Nam J, Xu R, et al. Impact of Contact Lens Zone Geometry and Ocular Optics on Bifocal Retinal Image Quality. Ophthalmic Physiol Opt 2014;34: 331–45.

50. Ruiz-Pomeda A, Perez-Sanchez B, Canadas P, et al. Binocular and Accommodative Function in the Controlled Randomized Clinical Trial MiSight® Assessment Study Spain (MASS). Graefes Arch Clin Exp Ophthalmol 2019;257:207–15.

51. Thibos LN, Bradley A, Liu T, et al. Spherical Aberration and the Sign of Defocus. Optom Vis Sci 2013;90: 1284–91.

52. Rose KA, Morgan IG, Ip J, et al. Outdoor Activity Reduces the Prevalence of Myopia in Children. Ophthalmology 2008;115:1279–85.

53. Wu PC, Tsai CL, Hu CH, et al. Effects of Outdoor Activities on Myopia among Rural School Children in Taiwan. Ophthalmic Epidemiol 2010;17:338–42.

54. Wu PC, Tsai CL, Wu HL, et al. Outdoor Activity during Class Recess Reduces Myopia Onset and Progression in School Children. Ophthalmology 2013;120: 1080–5.

55. Ravikumar S, Bradley A, Thibos LN. Chromatic Aberration and Polychromatic Image Quality with Diffractive Multifocal Intraocular Lenses. J Cataract Refract Surg 2014;40:1192–204.

56. Wallman J, Winawer J. Homeostasis of Eye Growth and the Question of Myopia. Neuron 2004;43:447–68.

57. Smith EL, 3rd, Hung LF, Huang J. Relative Peripheral Hyperopic Defocus Alters Central Refractive Development in Infant Monkeys. Vision Res 2009; 49:2386–92.

58. Flitcroft DI. The Complex Interactions of Retinal, Optical and Environmental Factors in Myopia Aetiology. Prog Retin Eye Res 2012;31:622–60.